

Observations of Nonlinear Effects in Directional Spectra of Shoaling Gravity Waves

M. H. FREILICH

Jet Propulsion Laboratory, California Institute of Technology, Pasadena

R. T. GUZA

Center for Coastal Studies, Scripps Institution of Oceanography, La Jolla, California

S. L. ELGAR

Electrical and Computer Engineering, Washington State University, Pullman

The spatial evolution of a directionally spread wave field on a near-planar natural beach is examined using data from longshore arrays of pressure sensors and wave staffs at 10.3 m and 4.1 m depth. High-resolution frequency-directional spectra from the deeper array are used to initialize a linear refraction model, and the resulting model predictions are compared with frequency-directional measurements at the shallow array. Linear theory inaccurately predicts both the shapes of directional spectra in shallow water and the total variances in some frequency bands. The discrepancies are largest for frequencies associated with maxima in the bicoherence spectrum, suggesting the importance of nonlinear effects. Furthermore, the measured directional spectrum at energetic low frequencies (0.05–0.11 Hz) and the vector resonance conditions for triads of long waves can be used to predict accurately the directions of observed peaks in directional spectra at higher frequencies (0.12–0.21 Hz). Prominent features in the measured directional spectra at the shallow array are thus consistent with energy transfers resulting from near-resonant triad interactions in the shoaling wave field.

1. INTRODUCTION

Nonbreaking water waves evolve substantially as they propagate shoreward in shallow water. As the depth decreases, wave amplitudes increase and initially symmetric wave profiles and oscillatory currents become asymmetric and skewed. Both linear and nonlinear processes act simultaneously to alter the frequency-directional characteristics of shoaling waves. The present study aims to identify qualitatively the nonlinear contribution to the shoaling transformation of frequency-directional spectra for natural waves propagating on a beach with nearly planar bathymetry.

Variations in water depth cause refraction, resulting in spatial changes in the amplitudes and directions of linear wave fields [e.g., *Longuet-Higgins*, 1957; *Collins*, 1972; *LeMéhaute and Wang*, 1982]. On most beaches, waves become more directionally collimated and amplitudes increase as the depth decreases. The linear refraction theory for wave fields that are broad in both frequency and direction has been developed extensively and applied to a variety of coastal surface wave studies, ranging from qualitative works [e.g., *Homma et al.*, 1966; *Wilson et al.*, 1973; *Pawka*, 1983] to numerical modeling of the full linear transformation of the frequency-directional spectrum by topography [e.g., *Pawka et al.*, 1984]. Linear theory has been reasonably successful in predicting directional characteristics of refracted waves in relatively shallow water, given estimates of deep water directional spectra and knowledge of the bathymetry.

However, it has long been recognized that linear refraction

theory is not uniformly valid. Even for initially infinitesimal waves normally incident on plane beaches, the linear theory predicts large wave amplitudes near the shore, thus violating the underlying assumption of linearity. When the initial wave field and/or the bottom topography varies spatially, linear refraction may predict the existence of caustic regions where the waves are neither slowly varying nor of small amplitude. Near such caustics, diffractive and nonlinear analyses are required (see *Peregrine and Smith* [1979, and references therein] for the cases of fully dispersive and nondispersive waves). While of fundamental importance for understanding interactions between dispersive waves and currents [*Peregrine and Smith*, 1979; *Peregrine and Thomas*, 1979], essentially monochromatic nonlinear analyses are not applicable to the shoaling region, where the wave fields are simultaneously weakly nonlinear, weakly dispersive, and broadbanded in frequency and (perhaps) direction.

On Pacific beaches, wind waves and swell in depths less than about 10 m are both weakly nonlinear and weakly dispersive. Near-resonant triad interactions can thus cause cross-spectral energy transfers and modal phase modifications as the waves propagate shoreward. *Freilich and Guza* [1984] (hereinafter FG) and *Liu et al.* [1985] (hereinafter LYK) have developed nonlinear shoaling models based on variants of the Boussinesq equations for long waves propagating in variable depth [*Peregrine*, 1972]. The models have no adjustable parameters, and the one-dimensional model of FG (which assumes that all waves are normally incident on a beach with no alongshore depth variations) has been successfully tested against extensive field observations on several beaches and for a variety of wave conditions [FG; *Elgar and Guza*, 1985a; *Elgar et al.*, 1990].

Copyright 1990 by the American Geophysical Union.

Paper number 90JC00354.
0148-0227/90/90JC-00354\$05.00

The most straightforward empirical search for nonlinear effects on the evolution of directional wave fields involves comparing measured frequency-directional spectra ($S(f, \theta)$) with the predictions of linear refraction theory. This requires measurements of $S(f, \theta)$ at two depths, since the data obtained in deeper water are used to initialize the linear refraction model. During a field experiment conducted in 1980, $S(f, \theta)$ was measured with two linear arrays of wave gages deployed at approximately 10 m and 4 m depths. The arrays were separated by 246 m in the cross shore, and the bottom topography between the arrays was smooth and nearly planar. The large alongshore extent of the arrays and the use of data adaptive processing techniques resulted in high directional resolution and accuracy over the wind wave frequency band.

In the case study reported here, 5 h of continuous data from the two directional arrays are used to show that nonlinear effects influence the evolution of the frequency-directional spectrum in the shoaling region, as suggested by the theoretical models of FG and LYK. Measurements at 10 m depth (and hence the predicted directional spectra at 4 m depth) were dominated by swell propagating from the south at low frequencies (<0.09 Hz) and by waves propagating from the north at higher frequencies. However, the measured two-dimensional spectra in shallow water showed evidence of significant southerly energy at harmonics of the incident swell that was not predicted by linear theory. In addition, linear theory did not predict observations of nearly normally incident energy found at the sum frequency of the south swell and the higher-frequency north "sea". These deviations between the measurements and the linear theory occurred at frequencies where the bicoherence was high, indicating significant nonlinear coupling within wave triads. Additionally, by using the bicoherence (to identify the frequencies of waves in a triad), the observed propagation directions for waves at two of the frequencies, and the vector resonance conditions presented by FG and LYK, the observed directions associated with apparently nonlinearly generated waves can be predicted accurately. The results presented for this particular subset of the data are also found to varying degrees in data obtained on many other occasions during this experiment.

The field experiment and data analysis are described in section 2. Measured frequency-directional spectra, and comparisons between predictions of linear refraction theory and data from the shallow array are presented in sections 3 and 4, respectively. Analyses of the discrepancies between measured shallow water directional spectra and those predicted by linear theory are given in section 5. Discussion and conclusions follow in section 6.

2. FIELD EXPERIMENT AND DATA ANALYSIS

Extensive measurements of shoaling waves collected throughout September 1980 at Torrey Pines Beach in southern California are described in detail in FG. Wave frequency-directional measurements for the present study were obtained from longshore arrays of six bottom-mounted pressure sensors (~ 10 m depth) and six surface-piercing wave staffs (~ 4 m depth) shown in Figure 1.

The offshore array (~ 10 m depth) was 395 m in total length. A five-sensor version of this array was established by Pawka [1982] and used for a series of investigations into the effects

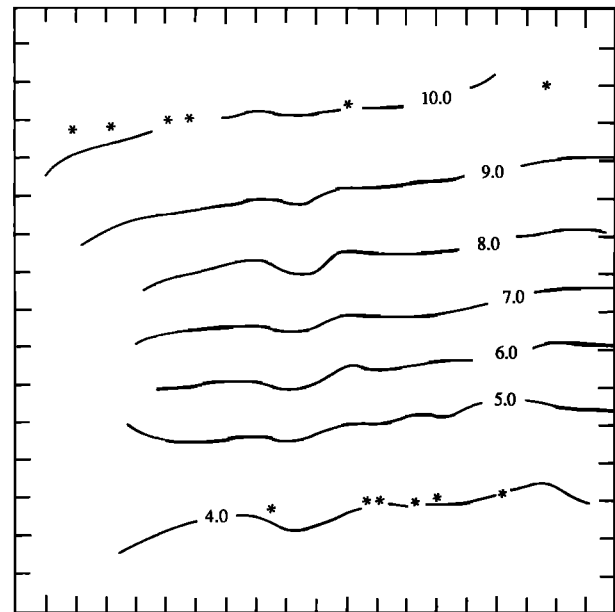


Fig. 1. Bathymetry at the Torrey Pines site, based on 1028 fathometer measurements obtained on September 9, 1980. Contour interval is 1 m. The locations of the sensors in the longshore arrays are denoted by asterisks. Ticks on axes are 25 m apart.

of island shadowing on the nearshore wave climate [Pawka, 1983; Pawka et al., 1984]. A sixth sensor added for the 1980 experiment increased the aliasing frequency to 0.20 Hz (cf. FG). Extensive testing by Pawka [1982, 1983] showed that the array could resolve bidirectional wave trains at $f = 0.067$ Hz separated by only 8° in direction (and varying significantly in relative amplitudes) when using maximum likelihood estimation. Greater angular resolution is achieved by using the iterative maximum likelihood estimation technique [Pawka, 1982, 1983; Oltman-Shay and Guza, 1984] described briefly below.

The shallow array was 192 m in longshore extent and was designed specifically to provide measurements of two-dimensional spectra for comparison with those measured at the deep array. Although the relative placements (longshore lags) of the wave staffs in the shallow array were not identical to those in the deep array, the shallow array had resolution comparable to that of the deep array after accounting for the effects of linear refraction. That is, if the deep array could resolve two wave trains that differed only slightly in direction, the shallow array could also resolve the wave trains assuming that the beach had parallel depth contours and that linear refraction theory was valid.

Figure 1 also shows the nearly planar bathymetry of the site, with depth contours based on a survey conducted on September 9, 1980 (within one day of acquiring the data presented below). Least squares fit of the tide-corrected depth measurements to a plane resulted in an on-offshore direction 264°T (i.e., the beach normal is $\sim 6^\circ$ south of west) and a mean slope of 0.02. The two arrays were very nearly aligned with the depth contours, with the axis of the deep array rotated 1° clockwise (i.e., 355°T) with respect to the depth contours, and the axis of the shallow array rotated 3° clockwise (357°T). In the following, all angles will be referred to an on-offshore coordinate system, with 0° corresponding to waves approaching normal to the beach, and

positive angles corresponding to waves approaching the beach from the north (angles greater than 264° T).

Data acquisition and calculation of Fourier coefficients of sea surface elevation are described in detail in FG. Time series of measurements every 0.5 s were constructed for each instrument by block averaging raw data sampled at 64 Hz. The time series were partitioned into 1024-s records and Fourier transformed. Where necessary, Fourier coefficients of near-bottom pressure were converted to coefficients of local sea surface elevation using the linear, finite-depth theory. For each record, the complex cross-spectral matrix between all sensors in a given directional array was averaged over eight frequency bands, yielding frequency resolution of 0.0078 Hz. The cross spectrum was then ensemble averaged over 20 records, resulting in estimates having 320 degrees of freedom.

At each frequency, high-resolution directional spectra were calculated from the averaged cross-spectral matrix and the known sensor positions using an iterative maximum likelihood (IMLE) technique [Pawka, 1983; Olman-Shay and Guza, 1984]. Starting with an initial maximum likelihood estimate of the directional spectrum [e.g., Davis and Regier, 1977], the IMLE method converges upon a possible true spectrum (i.e., one that can be used to retrieve the measured cross spectrum) by "unsmoothing" successive maximum likelihood estimates. The IMLE technique has been shown to yield accurate, high-resolution directional spectra from arrays and wave conditions that are very similar to those discussed here [Pawka, 1982, 1983].

3. MEASURED SPECTRA

In this study we analyze in detail a single 5-h period on September 10, 1980. The data were obtained on a falling tide, with a total depth change of 1 m over the 5 h. The mean depth was 10.33 m at the deep array and 4.12 m at the shallow array. Measured sea surface elevation variances were $\sim 360 \text{ cm}^2$ and $\sim 430 \text{ cm}^2$ at the deep and shallow arrays, respectively. Although similar directional measurements were obtained on 11 other occasions during the monthlong deployment, we present this particular data set because it exhibits a diversity of directional shoaling and refraction effects.

3.1. Frequency Spectra

One-dimensional frequency spectra measured at the center of each array and averaged over the entire 5 h are shown in Figure 2. At both array locations, the frequency spectrum is dominated by a narrow peak centered at 0.06 Hz. In 10 m depth, a broader peak extends from ~ 0.09 to 0.13 Hz. Less than 16% of the total variance is contributed by motions at frequencies greater than 0.13 Hz. Although the low-frequency swell peak is still present at the shallow array (4 m depth), the band 0.09–0.13 Hz now contains two significant peaks, centered at 0.10 Hz and at 0.12 Hz. Furthermore, although the spectrum continues to decrease at higher frequencies, there is a broad, low peak in the frequency range 0.16–0.20 Hz, centered near 0.18 Hz.

3.2. Frequency-Directional Spectra

IMLE estimates of frequency-directional spectra at the two arrays are shown in Figure 3. At 10 m depth (Figure 3a), virtually all of the observed wave energy is found within

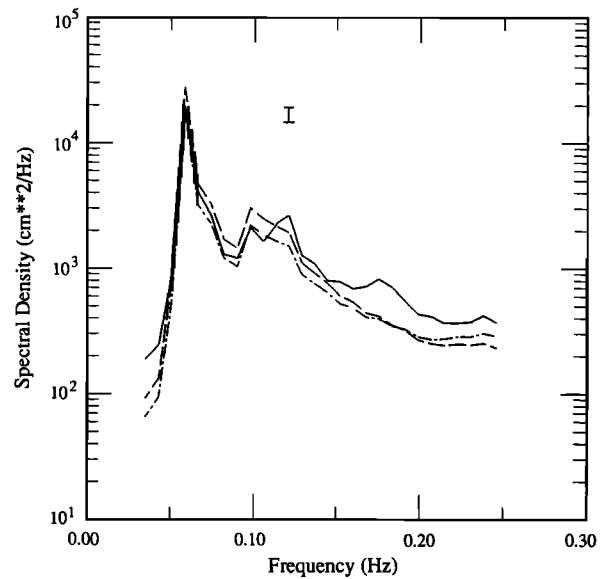


Fig. 2. Frequency spectra (320 degrees of freedom) of sea surface elevation for September 10, 1980. Shown are the measured spectrum at 10 m depth (dash-dot line), the prediction of LFDT at 4 m depth obtained by integrating (1) using the measured frequency-directional spectrum in 10 m depth (dashed line), and the measured spectrum at 4 m depth (solid line). Bar indicates 95% confidence interval for spectral estimates.

$\pm 25^\circ$ of normal incidence. The dominant low-frequency swell (0.05–0.09 Hz in Figure 2) is approaching the beach from the south (i.e., negative angular directions), and is bimodal with major and minor peaks centered at ($f = 0.06$ Hz, $\theta = -4^\circ$) and (0.08 Hz, -13°), respectively. For frequencies above ~ 0.09 Hz, most of the energy is approaching from the northern quadrant. In the frequency band 0.09–0.13 Hz, the waves are propagating primarily from the north (~ 2 – 17°), with the broadest distribution at the low-frequency end of this range. The frequency-directional data (Figure 3a) show that the single broad peak in the one-dimensional frequency spectrum at 0.09–0.13 Hz (Figure 2) is composed of waves propagating from both the northern and the southern quadrants.

The frequency-directional spectrum at the shallow array (Figure 3b) shows that the waves evolved significantly through the shoaling region. The peaks at the shallow array are typically narrower, of higher amplitude, and closer to the beach normal than are their counterparts at the deep array. Five distinct concentrations of variance are evident in Figure 3b: the low-frequency swell seen at the deep array, centered at $f = 0.06$ Hz and propagating from -4° (with a secondary maximum at $(\sim 0.08$ Hz, -8°); a broad peak with maximum at (0.10 Hz, $+10^\circ$); additional wave trains propagating from -4° at 0.12 Hz and 0.18 Hz; and a low peak centered at (0.16 Hz, $+6^\circ$). The three low-frequency maxima in the two-dimensional spectrum ($f = 0.06$, 0.10, and 0.12 Hz) correspond to the spectral peaks in the frequency spectrum (Figure 2) discussed above. The single, broad peak in the frequency spectrum ($f = 0.16$ –0.20 Hz) is evidently composed of two distinct wave trains, with the lower-frequency portion propagating from $+6^\circ$ and the higher-frequency portion from -4° .

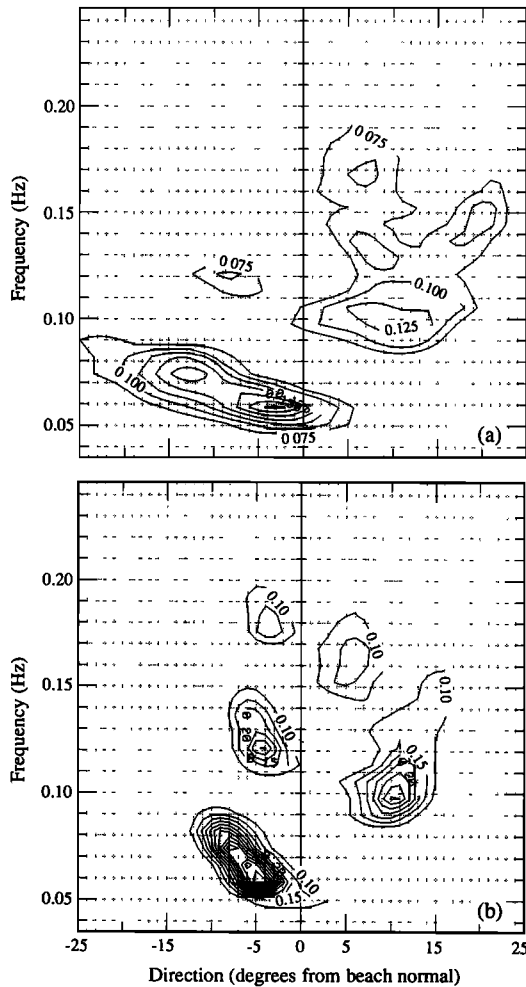


Fig. 3. Measured mean frequency-directional spectra: (a) 10 m depth; (b) 4 m depth. At each frequency, the variance is distributed linearly with direction while the total area under each curve is proportional to the logarithm of the autospectral density at that frequency. The frequency resolution is 0.0078 Hz.

4. COMPARISONS WITH PREDICTIONS OF LINEAR SHOALING THEORY

Linear, finite-depth theory (LFDT) can be used to estimate the transformation of the two-dimensional wave field between the deep and shallow arrays if the bottom slope is small, the waves neither gain energy (e.g., from the wind) nor lose energy through breaking and bottom friction, and if nonlinear effects are negligible. In the data considered here, the bottom slope is indeed small and input from the wind and losses resulting from bottom friction are expected to be negligible owing to the small (246 m) separation between the arrays. Wave breaking between the arrays was not visually apparent.

If the depth contours are everywhere straight and parallel, LFDT can be written as [LeMéhauté and Wang, 1982]

$$S(f, \theta) = \frac{kC_g}{k_0C_g} S_0 \left\{ f, \sin^{-1} \left[\frac{k}{k_0} \sin \theta \right] \right\} \quad (1)$$

where θ is the angle between the beach normal and the wave number vector \mathbf{k} , $k = |\mathbf{k}|$, $C_g \equiv (2\pi)\partial f/\partial k$ is the group speed, the dispersion relation is given by $(2\pi f)^2 = gk \tanh kh$

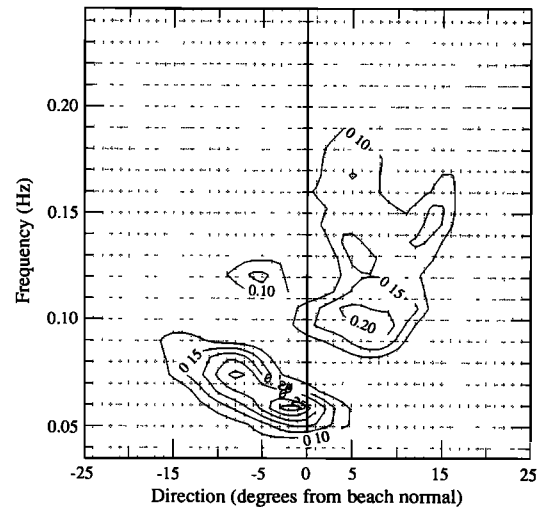


Fig. 4. Frequency-directional spectrum in 4 m depth predicted by LFDT using 10 m data as input. Contours are normalized as in Figure 3.

(where h is the depth), and the subscript zero refers to initial conditions (10 m depth in the present study).

An estimate of $S(f, \theta)$ at the shallow array calculated using (1) and the measured frequency-directional spectra from the deep array is shown in Figure 4. Directional spectra (one-dimensional slices through $S(f, \theta)$ at fixed frequencies) measured at 10 m depth and both measured and predicted (by LFDT) at 4 m depth are shown in Figures 5a-g.

The following comparisons between measurements and LFDT predictions focus primarily on the angular location of local maxima in the directional spectra ("peaks"), and the total autospectral levels in given frequency bands. These quantities, as well as approximate sea surface elevation variances associated with individual directional peaks, are summarized in Table 1 for the directional spectra shown in Figure 5.

Directional spectra of the dominant low-frequency south swell (0.06 Hz) and the north sea (0.10 Hz) are shown in Figures 5a and 5b, respectively. The directional spectra at both frequencies are essentially unimodal, and in each case LFDT overpredicts the total variance in the frequency band by approximately 30% and the refraction by about 2°. At $f = 0.07$ Hz (between the swell and the sea frequencies, and corresponding to a local minimum in the frequency spectrum), the directional spectrum is also unimodal and LFDT again overpredicts total variance (by 20%), but the direction of the peak is predicted to within 1° (Figure 5c).

Figures 5d-5g show more complex directional distributions caused by sheltering of the Torrey Pines site by offshore islands and banks [Pawka, 1983; Pawka et al., 1984]. Comparisons of predicted and measured shallow directional spectra at these frequencies reveal more significant discrepancies in both peak directions and total band variances. At $f = 0.12$ Hz (Figure 5d), the directional spectrum in 10 m depth is bimodal with peaks of nearly equal magnitude centered at -8° and $+11^\circ$. Linear shoaling would cause the amplitudes to increase comparably and the peaks to refract by about 3°. The measurements, however, show that the amplitudes and modal directions are not well predicted by LFDT. The observed northern peak contains approximately the predicted variance, but its apparent direc-

TABLE 1. Total Band Variances, Peak Directions, and Peak Variances for Directional Spectra in Figure 5

10-m Measured		4-m LFDT		4-m Measured	
Direction, deg	Variance, cm ²	Direction, deg	Variance, cm ²	Direction, deg	Variance, cm ²
			0.06 Hz		
-4	18684*	-2	27969*	-4	19568*
	17188		27703		17346
			0.07 Hz		
-13	2283*	-8	3285*	-8	2667*
	1913		2810		2247
			0.10 Hz		
+12	2203*	+8	3030*	+10	2122*
	1783		2471		1743
			0.12 Hz		
-8	1501*	-5	1921*	-4	2621*
+11	651	+8	844	+12	1488
	685		907		998
			0.14 Hz		
-5	750*	-3	912*	-6	1001*
+7	174	+5	217	...	476
+17	235	+12	288
	275		374	+14	528
			0.16 Hz		
-6	480*	-4	540*	...	689*
+7	104	+5	124	+6	...
+21	216	+15	248	+16	377
	126		162		167
			0.18 Hz		
-8	387*	-6	415*	-4	821*
+8	78	+6	87	+6	308
+15	168	+16	176	+16	266
	65		80		116

* Total variance in frequency band.

tion (+12°) is comparable to the unrefracted direction observed at the deep array. The observed southern peak is located at -4° (rather than the predicted -5°), but contains nearly twice the predicted variance. Overall, the measured autospectral density at this frequency exceeds the prediction of LFDT by a factor of 1.4, with nearly all of the discrepancy attributable to the large measured variance associated with the peak at -4°.

Figure 5e shows the directional spectrum at $f = 0.14$ Hz, near the high-frequency edge of the isolated directional peak at 0.11–0.15 Hz in Figure 3b. The most striking discrepancy between measured and predicted 4-m spectra is the hugely amplified southern peak that is observed, but is not well predicted by LFDT. The LFDT prediction of this peak is in error by more than a factor of 2 in variance and 3° in direction.

At $f = 0.16$ Hz (Figure 5f), both the 10-m measured spectrum and the LFDT prediction are trimodal as at 0.14 Hz, with predicted peaks in 4 m depth at -4°, +5°, and +15°. The shallow array data support the predictions for both the direction and the amplitude of the peak at +15°, but the southerly peak (predicted to be located at -4°) is not fully resolved. Most importantly, the measured directional spectrum is dominated by a peak centered at +6° and exceeding the LFDT prediction by a factor of 1.5 in variance.

The directional comparison at a relatively high frequency ($f = 0.18$ Hz) is shown in Figure 5g. Based on LFDT, the

directional spectrum at 4 m depth should be roughly trimodal, with minor peaks at -6° and +16°, and a larger, broad peak with maximum at +6°. The measurements confirm the minor peak at +16°, but show considerably larger peaks at +6° (underpredicted by LFDT by a factor of 1.5) and at -4° (underpredicted by a factor of 3.5). The total autospectral density in this band is underpredicted by LFDT by nearly a factor of 2.

The field data analyzed above suggest that at frequencies less than 0.12 Hz, LFDT predicts peak directions within a few degrees and total peak energies within about 30% (Figures 5a–5c). At higher frequencies, errors in LFDT predictions of both directions and variances are significantly larger. In particular, the linear theory inaccurately predicts the large peaks observed in the southern quadrant at 0.12 Hz and 0.14 Hz (Figures 5d and 5e), in the northern quadrant at 0.16 Hz (Figure 5f), and in both quadrants at 0.18 Hz (Figure 5g).

5. DISCREPANCIES BETWEEN LFDT AND DATA

In the previous section, predictions of directional spectra based on linear shoaling theory were seen to differ substantially from observations in 4 m depth. In the appendix, it is shown that the observed discrepancies are not primarily artifacts of the directional estimation technique. Other sources of error including depth variations during the run,

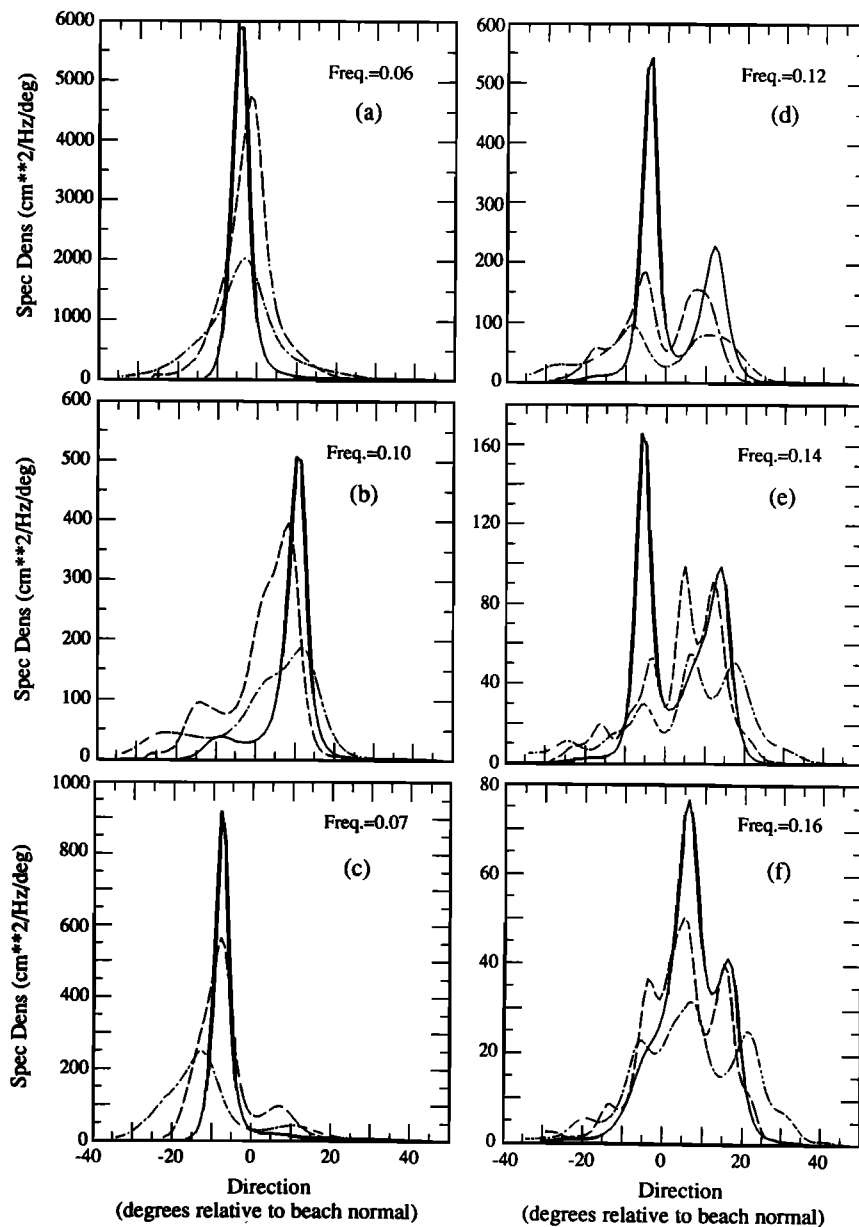


Fig. 5. Directional spectra at selected frequencies. Shown are measured spectra at 10 m depth (dash-dot lines), 4-m spectra predicted by LFDT based on 10-m measurements (dashed lines), and 4-m measurements (solid lines): (a) $f = 0.06$ Hz; (b) $f = 0.10$ Hz; (c) $f = 0.07$ Hz; (d) $f = 0.12$ Hz; (e) $f = 0.14$ Hz; (f) $f = 0.16$ Hz; (g) $f = 0.18$ Hz.

sensor placement errors, and data nonstationarity are believed to be relatively small. In this section, it is demonstrated that nonlinear wave-wave interactions can modify the amplitudes and directional distributions of shoaling wave fields to cause the discrepancies between LFDT and observations.

The shoaling models of FG and LYK suggest that wave transformation results from both linear conservation of energy flux and nonlinear, near-resonant triad interactions. The key requirement for near-resonant triad interactions is that both the frequencies and the vector wave numbers of the interacting waves must sum to (nearly) zero:

$$f_1 \pm f_2 \pm f_3 = 0 \tag{2a}$$

$$\mathbf{k}_1 \pm \mathbf{k}_2 \pm \mathbf{k}_3 = \mathbf{k}_\delta \quad |\mathbf{k}_\delta|/|\mathbf{k}_{1,2,3}| \ll 1 \tag{2b}$$

In one-dimensional comparisons with field data [e.g., FG; Elgar *et al.*, 1990], all waves were assumed to be propagating normal to a plane beach, so that (2b) reduced to a scalar equation relating the wave number magnitudes. Clearly, however, because (2b) is a vector equation, the near-resonant triad interactions can transfer energy across both frequencies (as in the one-dimensional model) and directions.

Elgar and Guza [1985b, 1986] and Doering and Bowen [1987] have used bispectral techniques to elucidate details of nonlinear triad interactions in the shoaling wave field. They showed that the bicoherence [Hasselmann *et al.*, 1963] could be used as a measure of nonlinear coupling between modes even for shoaling waves, where each mode is simultaneously participating in multiple near-resonant triads. Large bicoher-

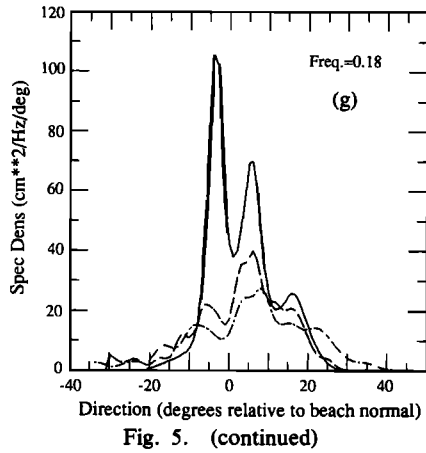


Fig. 5. (continued)

ence magnitudes indicated phase coupling between modes at different frequencies. Comparisons between data and the predictions of the FG model showed that for essentially narrow-banded wave fields such as the one considered in this study, small bicoherences indicated the absence of significant nonlinear interactions between the corresponding modes [Elgar and Guza, 1986].

Calculated bicoherences show, as expected, that nonlinearities in 4 m depth are stronger and more extensive than in 10 m depth in the present data set (compare Figures 6a and 6b). For most triads with all three component frequencies above 0.05 Hz (the low-frequency cutoff used in the directional analyses), bicoherence values at the deep array are insignificant, suggesting little nonlinear coupling. The isolated significant bicoherences involve the autospectral peak; the frequencies of the interacting waves are $(f_1 = 0.06, f_2 = 0.06)$, $(0.06, 0.08)$, and $(0.06, 0.12)$, with the convention that the third frequency of each triad is given by $f_3 = f_1 + f_2$.

In 4 m depth (Figure 6b), waves at the autospectral peak (~ 0.06 Hz) are significantly coupled to waves at all other frequencies, with particularly strong interactions at $(0.06, 0.06)$, $(0.06, 0.07)$, $(0.06, 0.12)$, and $(0.06, 0.16)$. Additional major nonlinear interactions are associated with the local bicoherence maxima at $(0.07, 0.12)$, $(0.09, 0.12)$, and $(0.11, 0.11)$.

As shown below, the major discrepancies between the observed and predicted frequency-directional spectra in 4 m depth occur at frequencies associated with bicoherence maxima (indicating significant nonlinear coupling), and the observed directions of anomalously energetic peaks are consistent with the vector resonance conditions (equation (2)).

5.1. Interactions Between the Autospectral Peak and Its Harmonics

The 4 m depth bicoherence maxima at $(0.06, 0.06)$ and $(0.06, 0.12)$ involve coupling of waves at the autospectral peak with themselves and their harmonics. The bicoherence peak at $(0.06, 0.06)$ is the self-self-second harmonic degenerate triad. In this case, (2) becomes

$$2f_1 - f_3 = 0 \quad (3a)$$

$$2\mathbf{k}_1 - \mathbf{k}_3 = \mathbf{k}_\delta \quad |\mathbf{k}_\delta| \ll |\mathbf{k}_{1,3}| \quad (3b)$$

If the bicoherence maximum is due to a near-resonant triad, (3b) must be satisfied. Physically, the wave number of the second harmonic must be oriented in nearly the same direction as \mathbf{k}_1 , and it must be nearly $2k_1$ in magnitude. From the linear, finite depth dispersion relation, $k_3/2k_1 = 1.07$ in 10 m depth, and the ratio decreases to 1.02 in 4 m as the waves become less dispersive. Figures 3b, 5a, and 5d show that the major directional peak at $f = 0.12$ Hz is indeed collinear with the peak at the primary frequency ($f = 0.06$ Hz). Furthermore, the observed concentration of variance at this direction is substantially underpredicted by linear shoaling theory (Figure 5d and Table 1).

Similar results hold for the bicoherence maximum at $(0.06, 0.12)$. In this case, $f_1 = 0.06$ Hz in (2a), $f_2 = 2f_1 = 0.12$ Hz, $f_3 = 0.18$ Hz, and the resulting triad consists of modes with frequencies corresponding to the primary and its first two harmonics. The dispersion relation yields $k_1 = 0.0585$ rad m^{-1} , $k_2 = 0.1236$ rad m^{-1} , and $k_3 = 0.1956$ rad m^{-1} in 4 m depth, so $k_3/(k_1 + k_2) = 1.07$. Considering first the directions of the largest peaks in the measured directional spectra, the resonance condition (2b) suggests that the primary ($f = 0.06$ Hz, $\theta = -4^\circ$) interacting with the (nonlinearly generated) second harmonic peak (0.12 Hz, -4°) should yield a directional peak at the third harmonic frequency (0.18 Hz) also at -4° . The interaction of the primary with the smaller amplitude peak in Figure 5d (0.12 Hz, $+12^\circ$) should result in a secondary directional peak at $(0.18$ Hz, $+7^\circ)$ if near-resonant triad interactions are significant. Peaks are, indeed, observed in the 0.18-Hz directional spectrum at -4° and $+7^\circ$, and the large peak amplitudes are not predicted by LFDT (Figure 5g).

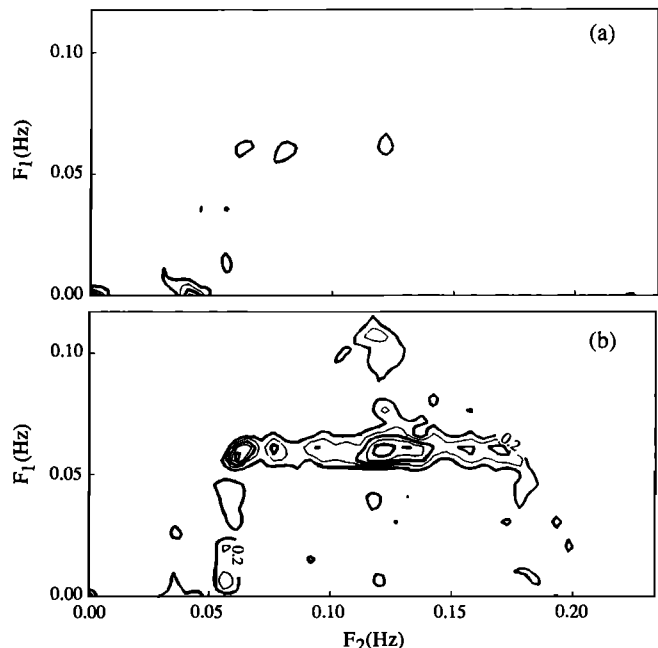


Fig. 6. Measured bicoherence spectra at (a) 10 m and (b) 4 m depths. Spectra have been averaged over 8×8 elementary frequency bands and 20 records. Nonsignificant bicoherence levels are not shown. Contour interval is 0.1, with even contours (above the 90% significance level) denoted by bold lines.

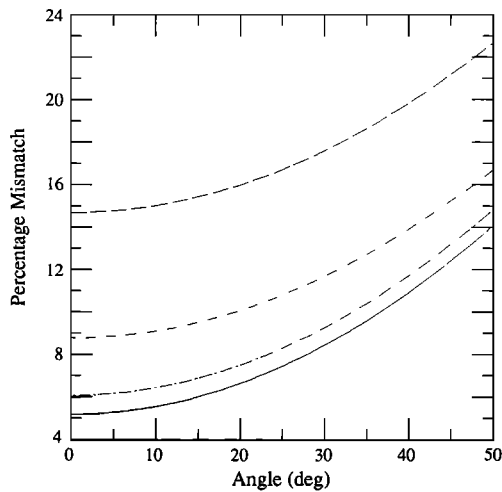


Fig. 7. Mismatch parameter (as defined in the text) at 7 m depth as a function of angle between the two lowest frequency waves in a triad. Solid line represents (0.06 Hz, 0.06 Hz, 0.12 Hz); long-dashed line, (0.10 Hz, 0.10 Hz, 0.20 Hz); dash-dot line, (0.06 Hz, 0.07 Hz, 0.13 Hz); and short-dashed line, (0.06 Hz, 0.10 Hz, 0.16 Hz).

5.2. Interactions Between the Primary and Nonharmonic Frequencies

The interactions between the autospectral peak and its harmonics discussed in section 5.1 primarily involve waves propagating in the same direction. For any given triad of frequencies obeying (2a), such “collinear” interactions guarantee minimum mismatch in the wave number resonance condition, since any mismatch results only from lowest-order dispersion. Interactions between waves propagating in different directions must result in larger wave number mismatches (and hence less net near-resonant energy transfers) because the magnitude of the vector sum wave number (k_3) must be smaller than required for a linear wave at the appropriate frequency. However, as noted in section 4, virtually all of the energy in the wind wave frequency band approached the beach within 25° of normal incidence, and the most energetic waves at 0.06 Hz were nearly normally incident (angles of about -4°). Wave number mismatch magnitudes (expressed as $1 - |\mathbf{k}_1 + \mathbf{k}_2|/k_3^{\text{lin}}$, where k_3^{lin} is the magnitude of the linear wave number at frequency f_3) are shown in Figure 7 for several different triads at 7 m depth. For all interactions discussed below, the mismatches are small and relatively insensitive to wave direction, so approach direction has only a small effect on the magnitudes of near-resonant transfers. In the present data set, the principal effect of the directionality in the incident wave field is on the directions (rather than the magnitudes) of the nonlinearly generated waves.

The third largest maximum in the bicoherence spectrum is located near (0.06, 0.08). It represents interactions between two wave trains propagating from the south, although in 4 m depth the higher-frequency waves are $\sim 4^\circ$ farther from normal incidence than are the primary waves. The nonlinearly generated waves should be observed at the sum frequency (about 0.14 Hz) and the vector sum direction (-6.2°). In fact, an anomalously large peak is observed at the proper direction in Figure 5e, and LFDT underpredicts its magnitude by nearly a factor of 2. Additional interactions between the primary and the more southerly swell at fre-

quencies around 0.08 Hz result in the elongated shape of the southern quadrant contours in the range 0.11–0.15 Hz in Figure 3b.

Of greater interest is the interaction at (0.06, 0.10) in Figure 6b, resulting in nonlinear energy transfers to waves with frequency 0.16 Hz. Figures 5a and 5b show that each of the two lower-frequency waves in the triad are nearly unimodal in direction, with the 0.06-Hz primary waves propagating from the south (-4°) and the 0.10-Hz waves approaching from the north ($+10^\circ$). The vector direction predicted by (2b) is $+4.8^\circ$, within one degree of the dominant peak observed in shallow water (Figure 5f and Table 1).

5.3. Interactions Away From the Autospectral Peak

Unfortunately, most of the identified bicoherence maxima not involving the energetic swell at 0.06 Hz result in nonlinear transfers to high-frequency waves ($f > 0.20$ Hz) which are directionally aliased by the deep array. Detailed comparisons between predictions of LFDT and measured spectra at 4 m depth are thus not possible. However, examination of Figure 3b at $f = 0.19$ Hz shows that a local directional maximum exists at $\theta = +6^\circ$, corresponding to the bicoherence maximum at (0.07, 0.12). The direction of the observed minor peak in the directional spectrum is consistent with a near-resonant triad interaction similar to those discussed above.

Although not apparent in Figure 3b, similar small peaks are observed at (0.22 Hz, $+3^\circ$) and (0.24 Hz, -3°). The first of these is consistent with interactions between the 0.10-Hz waves propagating from the north and the second harmonic (0.12 Hz) from the south, while the second peak is yet a higher harmonic of the primary, forced jointly by the self-self interaction of the second harmonic (0.12 Hz, 0.12 Hz) and the primary-third harmonic interaction (0.06 Hz, 0.18 Hz).

5.4. Discrepancies at $f = 0.06$ Hz and $f = 0.10$ Hz

As noted in section 4 (see Figures 5a and 5b), the observed directions of the south swell (0.06 Hz) and the north sea (0.10 Hz) did not agree with predictions of LFDT. In each case, the observed location of the directional peak in 4 m depth was 2° farther from normal incidence than predicted, and the low-frequency swell even appeared to have refracted away from normal incidence as the depth decreased.

The discrepancies are not readily attributed to uncertainties in array alignment or knowledge of the beach normal, since modal directions at frequencies away from the autospectral peaks and their harmonics are predicted well by LFDT (e.g., Figure 5c).

From the analysis above (and especially Figure 6b), it is clear that both the south swell and the higher-frequency north sea are participating in nonlinear, near-resonant triad interactions. As shown explicitly in FG and LYK, such interactions can result in modal phase modifications that can be interpreted as nonlinear changes to the wave number. Since the wave number magnitudes used in the calculations of directional spectra are determined by LFDT, the effective wave number magnitudes may differ from the predicted ones, thus contributing to discrepancies between the observed directional spectra and the predictions of LFDT. Additionally, the true local direction may indeed be altered by nonlinear effects.

5.5. The 10-m Directional Spectra

Nonlinearities in 10 m depth result in statistically significant bicoherences, although the bicoherence magnitudes are much smaller than those found in shallow water (compare Figures 6a and 6b). The bicoherence maxima in Figure 6a at (0.06, 0.06) and (0.06, 0.12) are the manifestations in 10 m depth of the harmonic interactions discussed in detail (for shallow water) in section 5.1. However, in 10 m depth the observed harmonic peak (0.12 Hz, -8°) is not precisely aligned with the fundamental ($\theta = -4^\circ$). The local maximum in the 10-m directional spectrum at 0.18 Hz ($\theta = -8^\circ$; Figure 5g) is also displaced from the primary. In 10 m depth, a significant fraction of the total energy at harmonic frequencies is from presumably free waves propagating from the north (cf. Figures 5d and 5g). Additionally, there is a 19% difference between the LFDT wave number used in the IMLE directional estimates and the wave number of waves at 0.18 Hz that are bound to, and forced by, the primary at 0.06 Hz. The relatively low energy levels in the southern quadrant and large wave number differences between bound and free waves could cause errors in the estimated directions of the harmonic peaks, thus resulting in the apparent misalignment.

Hasselmann *et al.* [1963] compared similar bispectral results in 11 m depth to the predictions of a nonresonant, second-order Stokes-type theory valid for small Ursell number. They noted agreement between observed and predicted bispectra. However, typical Pacific swell in 11 m depth has Ursell number ~ 0.3 , and the wave number mismatch parameter (section 5.2) between the primary and its second harmonic is small (~ 0.08). Swell waves in 10–12 m depth are thus in the transition region between nonresonant bound wave and near-resonant triad interactions, and neither theory is expected to be highly accurate. Had the Hasselmann *et al.* observations been obtained in 7 m depth (rather than 11 m), the agreement with nonresonant theory may not have been as good. The connection between shallow water, near-resonant Boussinesq theory, and nonresonant bound wave theory has not been fully explored, but is important in any model describing the propagation of nonlinear waves from deep to shallow water.

6. DISCUSSION AND CONCLUSIONS

Surface wave frequency-directional spectra ($S(f, \theta)$) measured in 4.1 m depth on a natural beach have been compared with the predictions of linear, finite-depth theory (LFDT; see equation (1)). Estimates of $S(f, \theta)$ measured in 10.3 m depth, 246 m seaward of the shallow array, were used to initialize the LFDT refraction model. The inadequacies of LFDT for the prediction of essentially one-dimensional quantities (i.e., Fourier coefficients of sea surface elevation at a point) are evident even in the autospectral comparisons (Figure 2), and have been well documented [e.g., Freilich and Guza, 1984; Elgar and Guza, 1985a, 1986]. The present study shows additionally that LFDT based on observations in 10 m depth cannot be used to predict accurately the directional distributions of shoaled waves in 4 m depth.

Freilich and Guza [1984] and Liu *et al.* [1985] have developed models describing the shoaling transformation as a combination of linear and nonlinear effects, the latter resulting from near-resonant triad interactions between

weakly dispersive waves. These models predict the nonlinear excitation of waves with frequencies and wave numbers satisfying triad near-resonance conditions (equations (2a) and (2b)). Consistent with the resonance conditions, a series of observed directional peaks at harmonic frequencies (e.g., $f = 0.12, 0.18, 0.24$ Hz) are aligned with the dominant south swell ($f = 0.06$ Hz, $\theta = -4^\circ$) in 4 m depth (Figures 3b, 5d, and 5g). Previous observations [Freilich and Guza, 1984; Elgar and Guza, 1985a] showing only directional alignment between the primary and its second harmonic were limited by array size and estimator resolution. In the present study, using better arrays and more sophisticated directional estimates, the alignment has been observed for the third and fourth harmonics, as well. For the first time, clear evidence has been presented for coupling between independent wave trains (e.g. 0.06 Hz and 0.10 Hz, and 0.06 Hz and 0.08 Hz) approaching the beach from different directions, with energy transferred to a third mode at the sum frequency and the vector sum direction as predicted by the resonance conditions.

Based on our analysis, an heuristic nonlinear “model” predicting the locations of directional peaks can be constructed when the autospectrum is dominated by a narrow, low-frequency swell, and the wind waves at frequencies less than twice the swell frequency have nearly unimodal directional distributions. Under these conditions, the dominant nonlinear triad sum interactions involve the waves at the autospectral peak. By assigning k_1 in (2b) to the vector wave number associated with the swell and similarly k_2 to the wave number of waves at each higher frequency, the resonance conditions (equation (2b)) yield the predicted peak vector wave number (and hence, direction) at the sum frequency. The “model” is thus valid for waves with frequencies exceeding twice the swell frequency.

Comparisons between these heuristic “predicted” directions and the observed peak directions at higher frequencies in 4 m depth are shown in Figure 8. With the exception of a single frequency just below the third harmonic of the swell, “predicted” and observed peak directions differ by at most 1° . The agreement is made even more remarkable by the fact that the observed peak directions vary by nearly 12° (and from southern to northern quadrants) across the frequency band 0.12–0.21 Hz (see Figure 3b).

The peak directions in 4 m depth predicted by LFDT are also shown in Figure 8. Although LFDT is reasonably accurate at frequencies less than the second harmonic of the swell, it is typically in error by more than 9° at higher frequencies. Curiously, at $f = 0.12, 0.16,$ and 0.17 Hz, LFDT appears to predict the observed peak direction to within 1° . The apparently accurate predictions of the linear model can be explained by the measured 10-m bicoherences in 10 m depth (Figure 6a). As discussed in section 5.5, significant bicoherence maxima are observed near (0.06, 0.06) and (0.06, 0.12), and nonlinearly generated waves nearly aligned with the swell are present even in the observed 10-m directional spectra. Thus, although the LFDT model based on the 10-m observations “correctly” predicts peak directions at discrete frequencies in shallow water, the directional spectra at those frequencies (see, for example, Figures 4, 5d, and 5f) show that LFDT underpredicts the amplitudes of the peaks in 4 m depth by nearly a factor of 2. The significant underprediction of peak amplitudes at those frequencies indicates that LFDT does not contain the essential physics

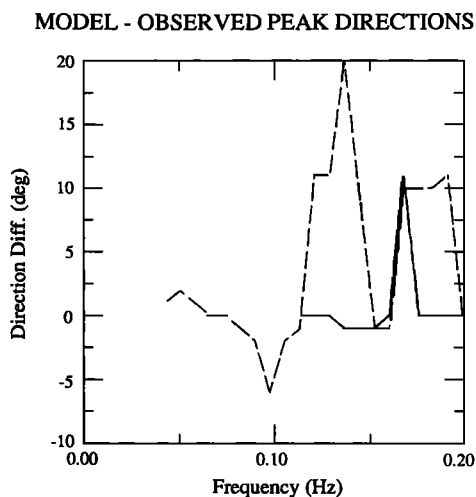


Fig. 8. Angular differences between predicted and observed peak directions ($\theta_{\text{pred}} - \theta_{\text{obs}}$) in 4 m depth. Solid line represents heuristic nonlinear "model" of section 6; dashed line, LFD T.

needed to predict wave shoaling, while Boussinesq models based on triad nonlinear interactions do.

In the data studied here, the peak directions in 4 m depth at frequencies between 0.12 and 0.21 Hz were determined primarily by nonlinear effects. Although full prediction of the two-dimensional spectrum (both directions and amplitudes at each frequency) requires application of a nonlinear two-dimensional shoaling model such as that of Liu *et al.* [1985], the present results clearly show that the effects of near-resonant triad interactions are detectable in field observations of frequency-directional spectra of shoaling waves.

APPENDIX: ESTIMATION ERRORS

Estimation of directional spectra from sparse longshore arrays as used in this study is not straightforward, and much effort in the past two decades has been expended to develop and test improved spectral estimation techniques. The IMLE technique used here (cf. section 2) was originally developed and tested using arrays and wave conditions at Torrey Pines that were very similar to those in this study [Pawka, 1982, 1983]. The technique is highly accurate for this particular situation and its performance is relatively insensitive to changes in initial conditions, array configurations, and choices of convergence parameters. Nonetheless, there is no mathematical formulation justifying IMLE, confidence levels on $S(f, \theta)$ are unknown, and the resulting estimated directional spectra are probably not even unique solutions. Although the present objective is to investigate shoaling waves (not to evaluate estimators), tests have been performed to eliminate the possibility that the "observed" directional spectra are primarily artifacts of the estimation process.

Two simulations were performed in which known directional spectra were used to generate noise-free cross-spectral matrices for a given array configuration. Directional spectra were then estimated from the simulated cross spectra and compared with the known inputs. In the first case, the inputs were taken to be the spectra at 4 m depth predicted by using deep array measurements and LFD T

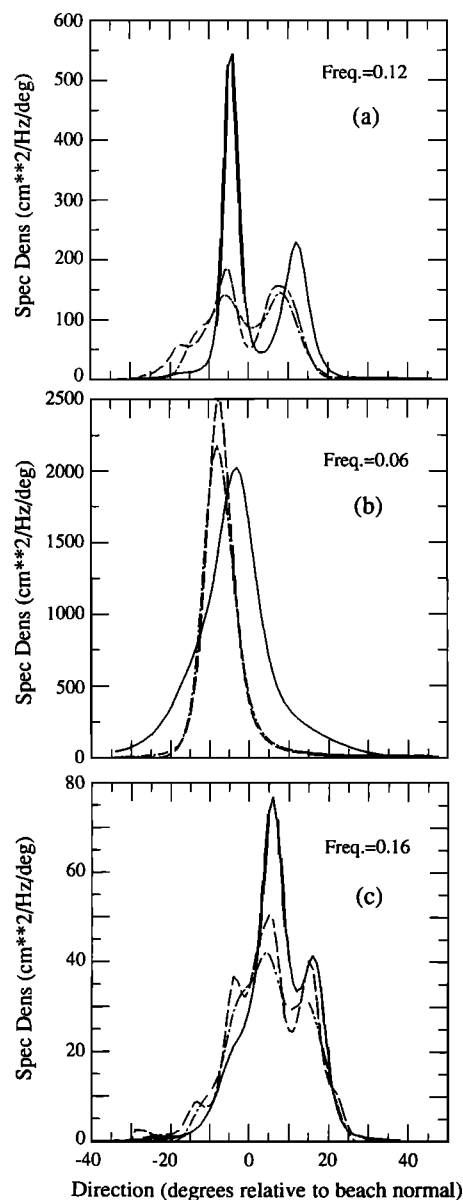


Fig. 9. Results of model tests of the arrays at selected frequencies. Shown on each panel are input spectra (dashed lines), output spectra (dash-dot lines), and measured spectra (solid lines). (a) Shallow array test at $f = 0.12$ Hz using as input the linear prediction in 4 m depth. (b) Deep array test at $f = 0.06$ Hz using as input the linear prediction at 10 m, based on the measured spectrum at 4 m depth. (c) Shallow array test at $f = 0.16$ Hz.

(i.e., the input spectra were the dashed lines in Figures 5a-5g). Cross spectra appropriate to the shallow array instrument locations were then generated, and the retrieved IMLE spectral estimates ("output spectra") were compared with the "input spectra." In similar fashion, measured shallow array spectra were used as input to (1), the resulting LFD T predictions at 10 m depth were used to generate the cross spectra at the deep array instrument locations, and output IMLE directional spectra were calculated. Examples at selected frequencies are shown in Figures 9a-9c. In each case, the discrepancies between input and output test spectra are small compared with the differences between the input (or output) and the measured spectra.

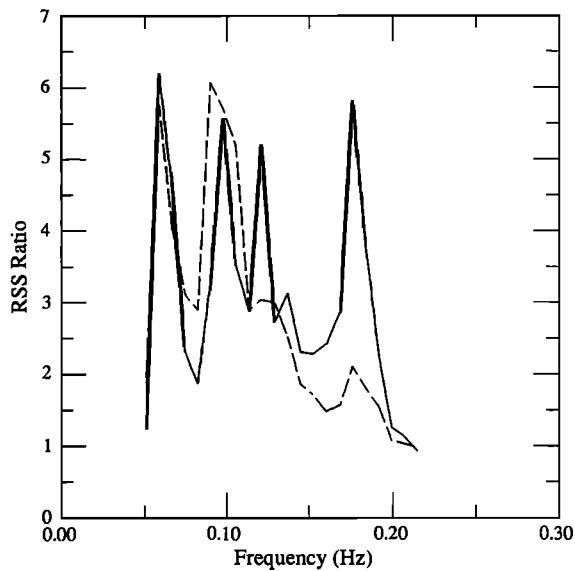


Fig. 10. Plots of $R(f)$ (equation (A1)) versus frequency for the test of the shallow array (solid line) and the deep array (dashed line).

Quantitative comparisons were obtained by calculating root-sum-square (rss) differences between input, output and measured directional spectra at each frequency. Denoting the input (derived from LFDT), measured (at 4 m or 10 m depth), and output (as described above) directional spectra by $S_i(f, \theta)$, $S_m(f, \theta)$, and $S_o(f, \theta)$ respectively, the rss difference ratio is given by

$R(f)$

$$= \left(\frac{\sum_{\theta} [S_m(f, \theta) - S_i(f, \theta)]^2}{\sum_{\theta} [S_o(f, \theta) - S_i(f, \theta)]^2} \right)^{1/2} \quad (\text{A1})$$

Large values of $R(f)$ result when the rss difference between a measured directional spectrum and the LFDT prediction is large compared with the "error" of the IMLE estimator.

Figure 10 shows $R(f)$ for both simulations. At all frequencies between 0.05 Hz and 0.21 Hz, $R(f) > 1$, indicating that deviations between the output spectra and the input (LFDT) spectra are small when compared with the deviations between measured and LFDT predicted spectra. Local maxima in $R(f)$ at 0.06, 0.10, 0.12, and 0.18 Hz correspond to the inaccurate predictions of LFDT shown in Figures 5a, 5b, 5d, and 5g. At 0.06 Hz and 0.10 Hz, the large errors result from small angular differences in the locations of the narrow unimodal peaks as discussed in section 5.4. At 0.12 Hz and 0.18 Hz, the shapes of input and output spectra differ qualitatively from the measured spectra owing to the nonlinear effects discussed in sections 4 and 5. At 0.16 Hz (Figure 5f), $R = 2.4$ for the shallow test; although significant differences between the measured directional spectrum and the simulated output are evident in Figure 9c (i.e., the large observed peak at $+6^\circ$), the magnitude of the rss ratio is not as large as at other frequencies. The above tests are neither as comprehensive nor as sophisticated as those of Pawka

cited above; however, the results imply that observed discrepancies between LFDT predictions and measured/estimated directional spectra result from the deficiencies in the LFDT model, and are not artifacts of the spectral estimation technique.

Acknowledgments. Portions of this analysis were conducted at the Jet Propulsion Laboratory, California Institute of Technology, under contract with NASA. Additional support for this work was provided by the Physical Oceanography program of the National Science Foundation (NSF). The data were acquired by the Center for Coastal Studies, Scripps Institution of Oceanography, during a field experiment supported by the Office of Naval Research (ONR). R. L. Lowe was principal engineer for the field experiment. T. H. C. Herbers made several helpful suggestions that improved the analysis.

REFERENCES

- Collins, J. I., Prediction of shallow water spectra, *J. Geophys. Res.*, **77**, 2693-2707, 1972.
- Davis, R. E., and L. A. Regier, Methods for estimating directional wave spectra from multi-element arrays, *J. Mar. Res.*, **35**, 453-477, 1977.
- Doering, J., and A. Bowen, Skewness in the nearshore zone: A comparison of estimates from Marsh-McBirney current meters and colocated pressure sensors, *J. Geophys. Res.*, **92**, 13,173-13,183, 1987.
- Elgar, S., and R. T. Guza, Shoaling surface gravity waves: Comparisons between field observations, linear theory, and a nonlinear model, *J. Fluid Mech.*, **158**, 47-70, 1985a.
- Elgar, S., and R. T. Guza, Observations of bispectra of shoaling surface gravity waves, *J. Fluid Mech.*, **161**, 425-448, 1985b.
- Elgar, S., and R. T. Guza, Nonlinear model predictions of bispectra of shoaling surface gravity waves, *J. Fluid Mech.*, **167**, 1-18, 1986.
- Elgar, S., M. H. Freilich, and R. T. Guza, Model-data comparisons of moments of nonbreaking shoaling surface gravity waves, *J. Geophys. Res.*, in press, 1990.
- Freilich, M. H., and R. T. Guza, Nonlinear effects in shoaling surface gravity waves, *Philos. Trans. R. Soc. London, Ser. A*, **311**, 1-41, 1984.
- Hasselmann, K., W. Munk, and G. MacDonald, Bispectra of ocean waves, in *Time Series Analysis*, edited by M. Rosenblatt, pp. 125-139, John Wiley, New York, 1963.
- Hom-ma, M., K. Horikawa, and Y. Chao, Sheltering effects of Sado Island on wind waves off Niigata Coast, *Coastal Eng. Jpn.*, **9**, 27-44, 1966.
- LeMéhauté, B., and J. D. Wang, Wave spectrum changes on sloped beach, *J. Waterw. Port Coastal Ocean Div. Am. Soc. Civ. Eng.*, **108**, 33-47, 1982.
- Liu, P.L.-F., S. B. Yoon, and J. T. Kirby, Nonlinear refraction-diffraction of waves in shallow water, *J. Fluid Mech.*, **153**, 185-201, 1985.
- Longuet-Higgins, M. S., On the transformation of a continuous spectrum by refraction, *Proc. Cambridge Philos. Soc.*, **53**(1), 226-229, 1957.
- Oltman-Shay, J., and R. T. Guza, A data-adaptive ocean wave directional spectrum estimator for pitch and roll type measurements, *J. Phys. Oceanogr.*, **14**, 1800-1810, 1984.
- Pawka, S. S., Wave directional characteristics on a partially sheltered coast, Ph.D. dissertation, 246 pp., Univ. of Calif. at San Diego, La Jolla, 1982.
- Pawka, S. S., Island shadows in wave directional spectra, *J. Geophys. Res.*, **88**, 2579-2591, 1983.
- Pawka, S. S., D. L. Inman, and R. T. Guza, Island sheltering of surface gravity waves: Model and experiment, *Cont. Shelf Res.*, **3**, 35-53, 1984.
- Peregrine, D. H., Equations for water waves and the approximations, behind them, in *Waves on Beaches and Resulting Sediment Transport*, edited by R. E. Meyer, pp. 95-122, Academic, San Diego, Calif., 1972.
- Peregrine, D. H., and R. Smith, Nonlinear effects upon waves near caustics, *Philos. Trans. R. Soc. London*, **292**, 341-370, 1979.

Peregrine D. H., and G. P. Thomas, Finite-amplitude deep water waves on currents, *Philos. Trans. R. Soc. London*, 292, 371-390, 1979.

Wilson, W. S., D. G. Wilson, and J. A. Michael, Analysis of swell near the island of Aruba, *J. Geophys. Res.*, 78, 7834-7844, 1973.

M. H. Freilich, Jet Propulsion Laboratory, California Institute of Technology, Pasadena, CA 91109.

R. T. Guza, Center for Coastal Studies, Scripps Institution of Oceanography, La Jolla, CA 92093.

S. L. Elgar, Electrical and Computer Engineering, Washington State University, Pullman, WA 99164.

(Received June 12, 1989;
accepted August 8, 1989.)